Calcium-activated chloride channels in the apical region of mouse vomeronasal sensory neurons

Michele Dibattista,[1] Asma Amjad,[1] Devendra Kumar Maurya,[1] Claudia Sagheddu,[1] Giorgia Montani,[2] Roberto Tirindelli,[2] and Anna Menini[1]

[1]Neurobiology Sector and Italian Institute of Technology Unit, Scuola Internazionale Superiore di Studi Avanzati (SISSA), 34136 Trieste, Italy

[2]Department of Neuroscience, University of Parma, and Brain Center for Social and Motor Cognition, Italian Institute of Technology, 43121 Parma, Italy

The rodent vomeronasal organ plays a crucial role in several social behaviors. Detection of pheromones or other emitted signaling molecules occurs in the dendritic microvilli of vomeronasal sensory neurons, where the binding of molecules to vomeronasal receptors leads to the influx of sodium and calcium ions mainly through the transient receptor potential canonical 2 (TRPC2) channel. To investigate the physiological role played by the increase in intracellular calcium concentration in the apical region of these neurons, we produced localized, rapid, and reproducible increases in calcium concentration with flash photolysis of caged calcium and measured calcium-activated currents with the whole cell voltage-clamp technique. On average, a large inward calcium-activated current of −261 pA was measured at −50 mV, rising with a time constant of 13 ms. Ion substitution experiments showed that this current is anion selective. Moreover, the chloride channel blockers niflumic acid and 4,4′-diisothiocyanatostilbene-2,2′-disulfonic acid partially inhibited the calcium-activated current. These results directly demonstrate that a large chloride current can be activated by calcium in the apical region of mouse vomeronasal sensory neurons. Furthermore, we showed by immunohistochemistry that the calcium-activated chloride channels TMEM16A/anoctamin1 and TMEM16B/anoctamin2 are present in the apical layer of the vomeronasal epithelium, where they largely colocalize with the TRPC2 transduction channel. Immunocytochemistry on isolated vomeronasal sensory neurons showed that TMEM16A and TMEM16B coexpress in the neuronal microvilli. Therefore, we conclude that microvilli of mouse vomeronasal sensory neurons have a high density of calcium-activated chloride channels that may play an important role in vomeronasal transduction.

The Journal of General Physiology

INTRODUCTION

Many social behaviors in animals are triggered by molecules with various chemical structures. In mammals, several chemosensory organs, such as the main olfactory epithelium, the vomeronasal organ (VNO), the septal organ, and the Grüneberg ganglion, are involved in chemical detection (Brennan and Zufall, 2006; Zufall and Leinders-Zufall, 2007; Brennan, 2009; Ma, 2009; Munger et al., 2009; Tirindelli et al., 2009; Touhara and Vosshall, 2009). Among these, the two main systems are represented by the main olfactory epithelium and the VNO. In both sensory systems, signal transduction occurs in bipolar sensory neurons and leads to membrane depolarization, although different transduction cascades are involved.

In most olfactory sensory neurons of the main olfactory epithelium, signal transduction occurs in the cilia protruding from the neurons' apical surface. The binding of molecules to odorant receptors leads to cAMP production and to the opening of CNG channels in the ciliary membrane. Na^+ and Ca^{2+} influx through CNG channels produces a depolarization of the neuron, and the increase in cytoplasmic Ca^{2+} concentration in the cilia has several effects, including a role in adaptation and the activation of Cl^- channels (Schild and Restrepo, 1998; Pifferi et al., 2006, 2009b; Kleene, 2008; Frings, 2009a,b; Reisert and Zhao, 2011).

In most vomeronasal sensory neurons, signal transduction occurs in microvilli that are present at the neurons' apical surface. The binding of molecules to vomeronasal receptors activates a phospholipase C signaling cascade, leading to the opening of ion channels that allow Na^+ and Ca^{2+} influx. The transient receptor potential canonical 2 (TRPC2) channel is expressed in the neurons' microvilli (Liman et al., 1999) and is mainly responsible for such cation influx (Zufall et al., 2005;

Correspondence to Anna Menini: menini@sissa.it

M. Dibattista's present address is Monell Chemical Senses Center, Philadelphia, PA 19104.

Abbreviations used in this paper: DAPI, 4′-6-diamidino-2-phenylindole; DIDS, 4,4′-diisothiocyanatostilbene-2,2′-disulfonic acid; MeS^-, methanesulfonate; NFA, niflumic acid; PDE4A, phosphodiesterase 4A; SCN^-, isothiocyanate; TRPC2, transient receptor potential canonical 2; VNO, vomeronasal organ.

The Rockefeller University Press $30.00
J. Gen. Physiol. Vol. 140 No. 1 3–15
www.jgp.org/cgi/doi/10.1085/jgp.201210780

Munger et al., 2009). Several studies demonstrated that vomeronasal sensory neurons respond to stimuli with the generation of action potentials and an increase in intracellular Ca^{2+} concentration (Holy et al., 2000; Leinders-Zufall et al., 2000, 2004, 2009; Spehr et al., 2002; Chamero et al., 2007). However, the role played by cytoplasmic Ca^{2+} elevation in the microvilli is still largely unknown. Spehr et al. (2009) have recently shown that Ca^{2+} in combination with calmodulin is responsible for sensory adaptation. In addition, other studies suggested that intracellular Ca^{2+} might also activate ion channels involved in the transduction process, although it is still a matter of debate whether these channels are cation or anion selective. Indeed, Ca^{2+}-activated nonselective cation currents have been measured in hamster (Liman, 2003) or mouse vomeronasal sensory neurons (Spehr et al., 2009). In the whole cell configuration, currents of about −177 pA at −80 mV were activated by dialysis of 0.5 or 2 mM Ca^{2+} (Liman, 2003). In excised inside-out patches, the dose–response relation indicated that half-activation of the channels occurred at 0.5 mM Ca^{2+} at −80 mV (Liman, 2003). It has been suggested that this Ca^{2+}-activated nonselective cation channel could directly mediate vomeronasal sensory transduction or amplify the primary sensory response (Liman, 2003), but at present its role and its molecular identity are still unknown. Other studies suggested that a significant portion of the response to urine in mouse vomeronasal sensory neurons is carried by Ca^{2+}-activated Cl^- channels (Yang and Delay, 2010; Kim et al., 2011). However, these studies used indirect ways to activate channels, as the increase in cytoplasmic Ca^{2+} concentration was a secondary effect of urine stimulation.

Thus, at present, it is still unclear whether nonselective cation and/or Cl^- channels activated by Ca^{2+} are expressed in the apical region of vomeronasal sensory neurons and may be involved in vomeronasal transduction. To contribute to the resolution of this debate, we directly recorded and characterized currents by producing rapid and repeatable increases in intracellular Ca^{2+} concentration using flash photolysis of caged Ca^{2+}, while recording the induced current in the whole cell voltage-clamp configuration (Boccaccio et al., 2011). The use of photolysis of caged Ca^{2+} to produce an increase in Ca^{2+} concentration, instead of dialysis of Ca^{2+} into the neuron or the production of a secondary Ca^{2+} increase, allowed us to release Ca^{2+} in a temporally and spatially defined manner into an intact neuron because we could precisely deliver a flash of UV light at the apical region of a vomeronasal sensory neuron. We measured an average inward Ca^{2+}-activated current of −261 pA at the holding potential of −50 mV and showed that this current is anion selective. Furthermore, both niflumic acid (NFA) and 4,4′-diisothiocyanatostilbene-2,2′-disulfonic acid (DIDS), two very well known Cl^- channel blockers (Frings et al., 2000; Hartzell et al., 2005), partially blocked the Ca^{2+}-activated current in vomeronasal sensory neurons.

To the best of our knowledge, these are the first recordings providing a direct demonstration that a large Cl^- current can be directly activated by Ca^{2+} in the apical region of mouse vomeronasal sensory neurons, as this demonstration can only be obtained by using a method that provides a temporal and spatial control of Ca^{2+} release, such as photolysis of caged Ca^{2+}.

Recent studies indicated that at least two members of the TMEM16/anoctamin family, TMEM16A/anoctamin1 and TMEM16B/anoctamin2, are Ca^{2+}-activated Cl^- channels (Caputo et al., 2008; Schroeder et al., 2008; Yang et al., 2008; Pifferi et al., 2009a, 2012; Stephan et al., 2009; Stöhr et al., 2009; Scudieri et al., 2012). We studied the expression of members of this family in the VNO and found that both TMEM16A and TMEM16B are expressed in the apical region of the VNO, in agreement with recent studies (Rasche et al., 2010; Billig et al., 2011; Dauner et al., 2012). However, microvilli both from vomeronasal sensory neurons and from supporting cells are present at the apical surface of the vomeronasal epithelium, and they are not clearly distinguishable. We therefore investigated the localization of TMEM16A and TMEM16B in isolated vomeronasal sensory neurons and found that these channels are expressed in neurons' microvilli. Because microvilli are the site where transduction events take place, the presence of Ca^{2+}-activated Cl^- channels indicates that they may be involved in signal transduction in the VNO. A complete understanding of conductances present in vomeronasal sensory neurons will help to elucidate the molecular mechanisms involved in the generation of the vomeronasal transduction current and the production of action potentials.

MATERIALS AND METHODS

Preparation of isolated vomeronasal sensory neurons

All animals were handled in accordance with the Italian Guidelines for the Use of Laboratory Animals (Decreto Legislativo 27/01/1992, no. 116) and European Union guidelines on animal research (no. 86/609/EEC). For experiments, 2-mo-old mice were anaesthetized by CO_2 inhalation and decapitated before VNO removal. The vomer capsule containing the VNO was removed as described previously (Liman and Corey, 1996; Dean et al., 2004; Shimazaki et al., 2006; Arnson et al., 2010), and vomeronasal sensory neurons were dissociated from the VNO with a standard enzymatic–mechanical dissociation protocol (Dibattista et al., 2008). In brief, the removed vomer capsule was rapidly transferred to a Petri dish containing divalent-free PBS (Sigma-Aldrich) solution where the VNO was extracted. The tissue was cut into small pieces with tiny scissors, transferred to divalent-free PBS containing 1 mg/ml collagenase (type A), incubated at 37°C for 10 min, cut into small pieces with tiny scissors, and reincubated for 10 min at 37°C. After a 2-min centrifugation at 1,700 rpm, the tissue was gently triturated with a fire-polished Pasteur pipette. Cells were resuspended in 1 ml of fresh Ringer's solution and plated on a glass coverslip (World Precision

Instruments) coated with poly-L-lysine and concanavalin A (type V; Sigma-Aldrich). Cells were stored at 4°C for up to 7 h before experiments.

Patch-clamp recordings

Vomeronasal sensory neurons were observed using an inverted microscope (IX 70; Olympus) with an oil immersion ×100 objective (Carl Zeiss). Currents in whole cell voltage-clamp configuration were recorded using an Axopatch 200B patch-clamp amplifier controlled by Clampex 8 connected with a Digidata 1322A (Molecular Devices). Patch pipettes were made using borosilicate capillaries (World Precision Instruments) and were pulled by a two-stage vertical puller (PP-83; Narishige). Pipette resistance was around 3–6 MΩ. Currents were low-pass filtered at 1 kHz and acquired at 2 kHz. All the experiments were performed at room temperature (20–24°C).

Ionic solutions, photolysis of caged Ca^{2+}, and perfusion system

The extracellular mammalian Ringer's solution contained (in mM): 140 NaCl, 5 KCl, 1 $CaCl_2$, 1 $MgCl_2$, 10 HEPES, 10 glucose, and 1 sodium pyruvate, pH 7.4. For flash photolysis of caged compounds, we used a xenon flash–lamp system (JML-C2; Rapp OptoElectronic) coupled with the epifluorescence port of the inverted microscope with a quartz light guide, as described previously (Boccaccio et al., 2006, 2011; Boccaccio and Menini, 2007). The light spot had a diameter of ∼15 µm and was focused on the microvilli and dendritic knob of isolated vomeronasal sensory neurons. The flash duration was <1.5 ms and was kept constant for each experiment. The interval between flashes was at least 2 min. At the beginning of each experiment, the stability of the response was checked by applying repetitive flashes at intervals of 2 min. Neurons that did not reach a stable response to at least two consecutive flashes were discarded.

The intracellular recording solution for the photorelease of caged Ca^{2+} contained (in mM): 3 DMNP-EDTA, 1.5 $CaCl_2$, 140 CsCl, and 10 HEPES, pH 7.4. DMNP-EDTA was purchased from Invitrogen, and $CaCl_2$ was adjusted with a 0.1-M standard solution from Fluka. Aliquots were stored at −20°C and kept refrigerated in the dark during the experiment.

For ionic selectivity experiments, NaCl was replaced with equimolar NMDG-Cl, or Cl^- was substituted with other anions, such as methanesulfonate (MeS^-) or isothiocyanate (SCN^-), by replacing NaCl on an equimolar basis with NaX, where X is the substituted anion.

The bath was grounded through a 1-M KCl agar bridge connected to an Ag-AgCl reference electrode. Liquid junction potentials were calculated using the Clampex's Junction Potential Calculator (Molecular Devices), based on the JPCalc program developed by Barry (1994), and applied membrane potentials were corrected offline for the calculated liquid junction potentials, as described previously (Sagheddu et al., 2010).

NFA was prepared in DMSO as stock solutions at 200 mM and diluted to the final concentration of 300 µM. DMSO alone did not modify the currents. DIDS was directly dissolved in the bathing solution to 1 mM.

Bathing solutions were changed by using a gravity-fed perfusion system with a slow perfusion rate, adjusted in such a way that the position of the neuron was not perturbed. A complete solution change was obtained in ∼10 s. To measure blocker effects, current recordings were obtained before blocker application until a stable response was obtained (control), 2 min after delivery of the solution with the blocker, and 2–5 min after perfusion with Ringer's solution without the blocker (wash).

Chemicals, unless otherwise stated, were purchased from Sigma-Aldrich.

Analysis of electrophysiological data

Data analysis and figures were made using Clampfit and IGOR software (WaveMetrics). Current recordings at each holding potential were plotted by subtracting the value of the baseline measured before photorelease of caged Ca^{2+}. Data are given as mean ± SEM and the total number of neurons (n). Statistical significance was tested with a Student's t test. $P < 0.05$ was considered statistically significant.

RNA extraction and RT-PCR

RNA was extracted from the VNO of FVB mice. Methods and primers for the amplification of TMEM16/anoctamins cDNA were the same as described previously (Sagheddu et al., 2010). All amplicons were gel extracted, subcloned, and sequenced for confirmation.

Immunofluorescence

HEK 293T cells were grown on coverslips and cotransfected with plasmids containing the cDNA sequence of TMEM16A or TMEM16B (RZPD) and enhanced GFP (Takara Bio Inc.) for fluorescent identification of transfected cells, as described previously (Pifferi et al., 2009a). Transfected cells were fixed in 4% paraformaldehyde for 15 min at room temperature and sequentially washed. Next, they were incubated with a quenching solution (0.1 M glycine) for 10 min and then treated with 0.05% SDS for antigen retrieval for 10 min. Cells were subsequently incubated for 15 min in blocking solution (2% [vol/vol] FBS and 0.2% [vol/vol] Triton X-100 in PBS), followed by incubation with the primary antibody for 3 h at 4°C. After washing with PBS-T (0.1% Tween 20 in PBS), cells were incubated for 45 min with the secondary antibody, prepared in PBS-T. Finally, cells were incubated with 0.1 µg/ml 4′-6-diamidino-2-phenylindole (DAPI) for 15 min, and coverslips were mounted with Vectashield (Vector Laboratories).

For immunohistochemistry on tissue sections, the mouse nasal regions or the VNOs extracted from the nasal cavity were fixed in 4% paraformaldehyde (for 4 h at 4°C), then decalcified in 0.5 M EDTA for 12 h at 4°C, and subsequently equilibrated overnight (4°C) in 30% (wt/vol) sucrose for cryoprotection. 14-µm coronal sections were cut with a cryostat and stored (−80°C) for further use. For antigen retrieval, sections were treated with SDS 0.5% (wt/vol) in PBS for 15 min. Sections were incubated in a blocking solution (2% [vol/vol] FBS and 0.2% [vol/vol] Triton X-100 in PBS) for 2 h, and then with the primary antibody (diluted in the blocking solution) overnight at 4°C. Sections were then rinsed with 0.1% (vol/vol) Tween 20 in PBS (PBS-T) and incubated with the fluorophore-conjugated secondary antibody (diluted in PBS-T) for 2 h at room temperature. After washing with PBS-T, sections were treated with 0.1 µg/ml DAPI for 30 min, washed with PBS-T, and mounted with Vectashield (Vector Laboratories).

Immunocytochemistry on isolated vomeronasal sensory neurons was performed as described previously (Fieni et al., 2003). Dissociated vomeronasal sensory neurons were prepared as for electrophysiological experiments. Glass-attached vomeronasal neurons were gently perfused with 4% paraformaldehyde and then washed in PBS. Cells were blocked in 1% albumin and 0.3% Triton X-100 in PBS for 20 min and incubated overnight with the primary antibody. Cells were then washed in PBS and further incubated with the secondary antibody, prepared in PBS. In some experiments, cells were also incubated with 0.1 µg/ml DAPI for 15 min. Coverslips were mounted with Vectashield (Vector Laboratories).

Wild-type C57BL6 or genetically modified mice that express GFP in all mature olfactory and vomeronasal sensory neurons (OMP-GFP mice; provided by P. Mombaerts, Max Planck Institute of Biophysics, Frankfurt, Germany) were used.

The following primary antibodies were used: rabbit anti-TMEM16A (1:50; Abcam), rabbit anti-TMEM16B (1:100; Santa Cruz Biotechnology, Inc.), guinea pig anti-TMEM16A and guinea

pig anti-TMEM16B (provided by S. Frings, Heidelberg University, Heidelberg, Germany; Dauner et al., 2012), goat anti-TRPC2 (1:50; Santa Cruz Biotechnology, Inc.), rabbit anti-Gαo (1:100; Santa Cruz Biotechnology, Inc.), and rabbit anti–phosphodiesterase 4A (PDE4A; 1:50; Abcam). The following secondary antibodies, obtained from Invitrogen, were used: goat anti–guinea pig Alexa Fluor 594 (1:500), goat anti–rabbit Alexa Fluor 488 (1:500), goat anti–rabbit Alexa Fluor 594 (1:500), goat anti–rabbit Alexa Fluor 405 (1:500), chicken anti–rabbit Alexa Fluor 594 (1:500), and chicken anti–goat Alexa Fluor 488 (1:500).

Immunoreactivity was visualized with a confocal microscope (TCS SP2; Leica). Images were acquired using Leica software (at 1,024 × 1,024–pixel resolution) and were not modified other than to balance brightness and contrast. Control experiments without the primary antibodies gave no signal.

RESULTS

Whole cell currents activated by photolysis of caged Ca^{2+} at the apical region of mouse vomeronasal sensory neurons

We obtained whole cell voltage-clamp recordings from isolated mouse vomeronasal sensory neurons and directly measured Ca^{2+}-activated currents by rapidly elevating the Ca^{2+} concentration in the apical region (dendritic knob and microvilli) by localized photorelease of caged Ca^{2+} (Fig. 1 A). Fig. 1 B shows a typical current response at the holding potential of −50 mV. An inward current rapidly developed upon the flash release, reaching a peak amplitude of −508 pA, and then slowly returned to baseline. The rising phase of the Ca^{2+}-activated current was well described by a single-exponential function with a time constant of 9.5 ms (Fig. 1 C). Similar results were obtained from a total of 59 neurons with an average time constant value of 12.6 ± 6.0 ms (n = 59; range of 3–26 ms). We observed a large variability in Ca^{2+}-activated current amplitudes in different neurons with absolute values ranging between 50 pA and 1 nA at −50 mV, and a mean amplitude of −261 ± 37 pA (n = 59). Such variability has also been observed in recording Ca^{2+}-activated currents in the ciliary region of olfactory sensory neurons, where absolute values ranging from 50 pA up to ∼1 nA were also recorded (Boccaccio et al., 2006; Boccaccio and Menini, 2007). The amplitude variability can originate both from the illumination conditions in the neuron that may differ between experiments as well as from various numbers or densities of channels that may vary in different neurons. Similarly to olfactory sensory neurons, we also found a large variability in the time necessary for the current to return to baseline in vomeronasal sensory neurons (Figs. 1 B and 3, A and B). This is likely to be the result of differences in the time necessary for the decrease in Ca^{2+} concentration by Ca^{2+} extrusion and/or by diffusion to other neuronal compartments.

To investigate the ionic nature of the Ca^{2+}-activated currents, we measured the reversal potential in various ionic conditions. Currents were recorded at various holding potentials with different ionic compositions in the extracellular solution. In a first set of experiments, we used our standard intracellular and extracellular solutions, in which Cs^+ was chosen as the intracellular monovalent cation to avoid contributions from Ca^{2+}-activated K^+ currents, and Na^+ was the main extracellular monovalent cation. Moreover, the intracellular and extracellular Cl^- concentrations were almost symmetrical. Fig. 2 A shows the responses induced by photorelease of Ca^{2+} at the indicated holding potentials. The reversal potential calculated from the current–voltage relation was +0.5 mV, with an average value of +0.3 ± 3.5 mV (n = 6; Fig. 2 E). Because the cation concentrations were $[Na^+]_o$ = 149 mM and $[Cs^+]_i$ = 143 mM, and the Cl^- concentrations were $[Cl^-]_o$ = 149 mM and $[Cl^-]_i$ = 143 mM, a reversal potential value close to 0 mV is consistent both with a nonselective cation current and with an anion-selective current.

To distinguish between the two types of currents, we performed a first set of experiments by replacing Na^+ in the extracellular solution with $NMDG^+$, a large organic monovalent cation largely impermeant in cation channels. If the measured Ca^{2+}-activated currents were carried by cations, the replacement of Na^+ by $NMDG^+$ should produce a shift of the reversal potential toward negative values. Fig. 2 B shows that the reversal potential in the presence of 140 mM NMDG-Cl was +0.3 mV, with an average value of +0.5 ± 3.8 mV (n = 3; Fig. 2 E), indicating that the Ca^{2+}-activated current was not carried by cations.

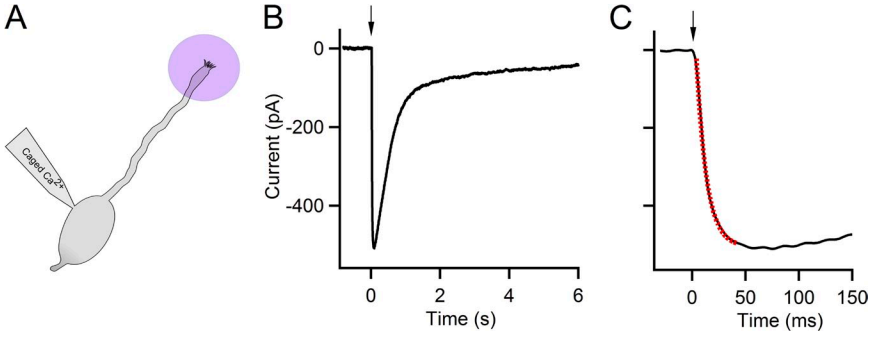

Figure 1. Current responses induced by photorelease of Ca^{2+} in the apical region of mouse vomeronasal sensory neurons. (A) Schematic drawing of a vomeronasal sensory neuron showing the location of application of the UV flash to photorelease Ca^{2+}. (B) Whole cell current induced by photorelease of Ca^{2+} at the holding potential of −50 mV. A flash was applied at time t = 0 (indicated by an arrow). (C) Expanded timescale shows the rapid increase in the current upon Ca^{2+} photorelease. The current rising phase was well fitted by a single exponential (red dotted line) with a τ value of 9.5 ms.

In a second set of experiments, we tested whether the Ca^{2+}-activated current was carried by Cl^- by substituting most of the extracellular Cl^- with MeS^-, an anion known to be almost impermeant in Cl^- channels. Fig. 2 C shows that, when we replaced 140 NaCl with NaMeS, the reversal potential was +18 mV, with an average value of +20.2 ± 1.5 mV (n = 3; Fig. 2 E). The average reversal potential in the low extracellular Cl^- solution was shifted toward more positive values, as expected if MeS^- is much less permeant than Cl^-. Furthermore, because most Cl^- channels are more permeable to SCN^- than to Cl^-, we measured the reversal potential after replacing 140 mM NaCl with NaSCN: the reversal potential shifted toward more negative values, −20 mV (Fig. 2 D), with an average value of −18 ± 3 mV (n = 8; Fig. 2 E). These results demonstrate that the Ca^{2+}-activated current is an anion current and that these ion channels have higher permeability for SCN^- over Cl^-, as in most Cl^- channels (Hartzell et al., 2005).

To further characterize these channels, we measured the extracellular blockage by NFA and DIDS, two compounds commonly used to partially block Ca^{2+}-activated Cl^- currents in various tissues (Frings et al., 2000). Fig. 3 A shows the blocking effect by 300 µM NFA of the current elicited by photolysis of caged Ca^{2+} at −50 mV. The maximal inward current decreased from −1,022 to −221 pA upon NFA application, corresponding to 22% of its value before blocker application. The blocking effect was partially reversible after perfusion with Ringer's solution without NFA, as the current amplitude recovered to −505 pA, 50% of the control value. On average, the current amplitude in the presence of 300 µM NFA at −50 mV was 27% (n = 5) of the value before blocker application (Fig. 3 C). After perfusion with Ringer's

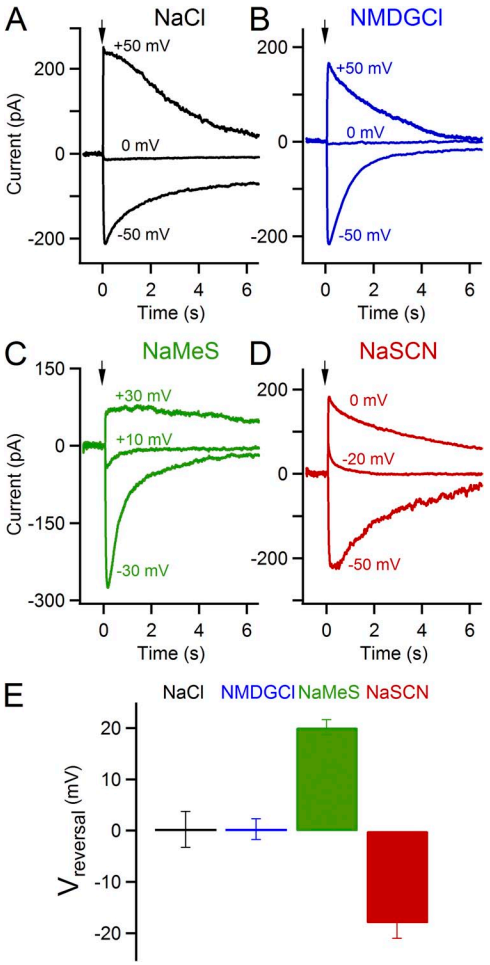

Figure 2. Ion selectivity of the Ca^{2+}-activated current. Whole cell currents from vomeronasal sensory neurons induced by photorelease of Ca^{2+} into the apical region recorded at the indicated holding potentials. A UV flash was applied at the time t = 0 (indicated by an arrow). Recordings in the presence of extracellular Ringer's solution containing 140 mM: (A) NaCl, (B) NMDG-Cl, (C) NaMeS, and (D) NaSCN, each from a different neuron. (E) Average reversal potentials measured in the presence of the indicated ionic solutions: NaCl (n = 6), NMDG-Cl (n = 3), NaMeS (n = 3), and NaSCN (n = 8).

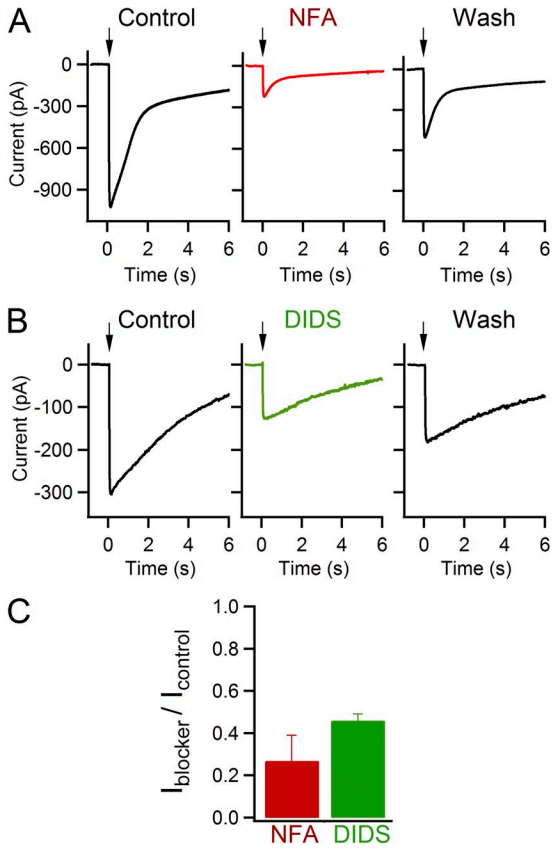

Figure 3. Blockage of the Ca^{2+}-activated Cl^- current. Whole cell currents induced by photorelease of Ca^{2+} into the apical region of vomeronasal sensory neurons. The holding potential was −50 mV. Current recordings were obtained before blocker application (control), 2 min after application of the indicated blockers, and 2 min after the removal of blockers (wash). The following blockers were used: (A) 300 µM NFA and (B) 1 mM DIDS. (C) Average values of the current in the presence of 300 µM NFA (n = 5) or 1 mM DIDS (n = 3) normalized to the current in control conditions ($P < 0.05$).

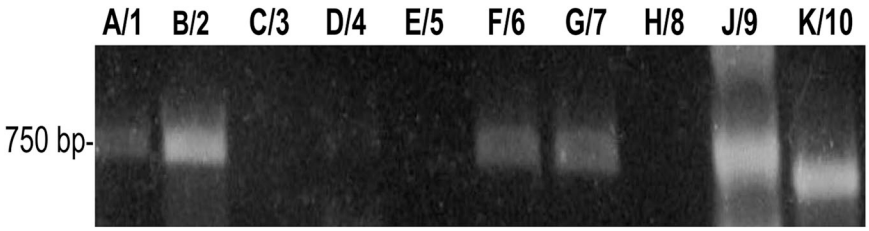

Figure 4. Expression of TMEM16s/anoctamins in mouse VNO. TMEM16/anoctamin isoforms A–J (1–10) were amplified from VNO cDNA by RT-PCR. A/1, B/2, F/6, G/7, J/9, and K/10 are expressed in the VNO.

solution without the blocker, the current recovered on average to 68% of its control value.

Fig. 3 B shows recordings from a vomeronasal sensory neuron in which the extracellular addition of 1 mM DIDS produced a block to 42% of its control value. After washout with Ringer's solution, the current amplitude reached 60% of the value before blocker application. On average, the current amplitude in the presence of 1 mM DIDS was 46% ($n = 3$) of the control value (Fig. 3 C). After perfusion with Ringer's solution without DIDS, the current was on average 60% of its control value.

Collectively, these results show that a sudden increase in the intracellular Ca^{2+} concentration can rapidly activate a large anion current, demonstrating the expression of a high density of Ca^{2+}-activated Cl^- channels in the apical region of vomeronasal sensory neurons.

Expression of TMEM16s/anoctamins in mouse VNOs

Having measured Ca^{2+}-activated Cl^- currents in the apical region of mouse vomeronasal sensory neurons, we sought to investigate which members of the TMEM16/anoctamin family that are known to function as Ca^{2+}-activated Cl^- channels are expressed in the VNO.

To analyze the expression of each TMEM16/anoctamin, we performed RT-PCR on cDNA obtained from mouse VNOs. mRNAs of TMEM16A/anoctamin1, B/2, F/6, G/7, J/9, and K/10 were found to be significantly expressed in the VNO (Fig. 4).

Because antibodies against TMEM16A and TMEM16B are commercially available, we first tested their specificity on HEK 293T cells transiently transfected with plasmids containing the cDNA sequence of TMEM16A or TMEM16B and GFP. Fig. 5 shows that cells transfected with TMEM16A (Fig. 5, A–F) or TMEM16B (Fig. 5, G–L)

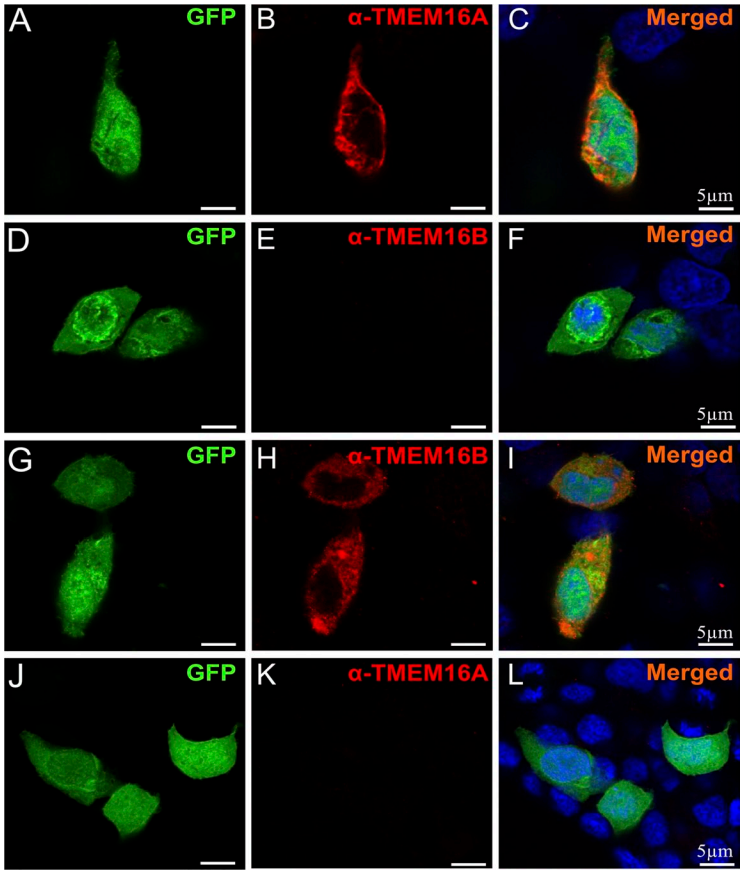

Figure 5. Specificity of rabbit anti-TMEM16A and anti-TMEM16B antibodies in HEK 293T cells expressing TMEM16A or TMEM16B. (A–F) Fluorescence images of the staining with anti-TMEM16A or anti-TMEM16B antibodies (indicated with the prefix α) of HEK 293T cells transiently cotransfected with TMEM16A and GFP cDNA. Specific staining was observed only with anti-TMEM16A (B), whereas no immunoreactivity was detected with anti-TMEM16B (E) antibody. (G–L) Fluorescence images of the staining with anti-TMEM16B or anti-TMEM16A antibodies of HEK 293T cells transiently cotransfected with TMEM16B and GFP cDNA. Specific staining was observed only with anti-TMEM16B (H), whereas no immunoreactivity was detected with anti-TMEM16A (K) antibody. Cell nuclei were stained by DAPI (blue). Bars, 5 µm.

cDNA produced a strong and specific immunoreactivity exclusively to their respective antibody.

We further investigated the specificity of the two antibodies on the olfactory epithelium. Indeed, it is well established that TMEM16B is expressed in the apical layer of the olfactory epithelium but not in the respiratory epithelium (Hengl et al., 2010; Rasche et al., 2010; Billig et al., 2011). We used genetically modified OMP-GFP mice that express GFP in all mature olfactory and vomeronasal sensory neurons (Potter et al., 2001) and confirmed that TMEM16B was expressed at the apical surface of the olfactory epithelium but not in the respiratory epithelium (Fig. 6, D–F), and that TMEM16A immunoreactivity was absent (Fig. 6, A–C). Collectively, these experiments indicate that these antibodies specifically recognized their epitopes and did not show cross-reactivity.

We therefore used the same antibodies to examine the localization of TMEM16A and TMEM16B in the vomeronasal epithelium of OMP-GFP mice and detected immunoreactivity at the luminal surface of the sensory epithelium (Fig. 7, A–F). High magnification images show that both anti-TMEM16A (Fig. 7 G) and anti-TMEM16B (Fig. 7 H) staining lies above the knobs of the vomeronasal sensory neurons, where microvilli are located. We also costained VNO sections with an antibody against the cation channel TRPC2, which is involved in vomeronasal transduction, and observed staining in the microvillar region (Fig. 8, B and E) that largely colocalized with TMEM16A and TMEM16B immunoreactivity (Fig. 8, A, C, D, and F), indicating that cation (TRPC2) and anion channels (TMEM16A and TMEM16B) coexpress. However, the microvillar region is composed of microvilli of both sensory neurons and supporting cells (Höfer et al., 2000; Dauner et al., 2012), and they cannot be distinguished in immunosignals from VNO coronal sections.

To unequivocally establish whether TMEM16A and/or TMEM16B are expressed in the microvilli of sensory neurons, the compartment responsible for signal transduction, we performed immunocytochemistry on isolated vomeronasal sensory neurons using combinations of the commercially available antibodies raised in rabbit and of those raised in guinea pigs (provided by S. Frings; Dauner et al., 2012). Figs. 9 and 10 illustrate that TMEM16A and TMEM16B are both expressed in the microvilli of vomeronasal sensory neurons. Moreover, Fig. 9 clearly shows the coexpression of TMEM16A and TMEM16B in the microvilli of the same neuron from an OMP-GFP mouse. After dissociation and immunocytochemistry procedures, we obtained 34 intact isolated vomeronasal sensory neurons from four OMP-GFP mice, and 62 intact neurons from 10 wild-type mice. Every intact vomeronasal sensory neuron, both from OMP-GFP and wild-type mice, showed coexpression of TMEM16A and TMEM16B in the microvilli. For coexpression, both combinations of rabbit anti-TMEM16A with guinea pig anti-TMEM16B and guinea pig anti-TMEM16A with rabbit anti-TMEM16B produced the same result. Unfortunately, in our preparation of dissociated

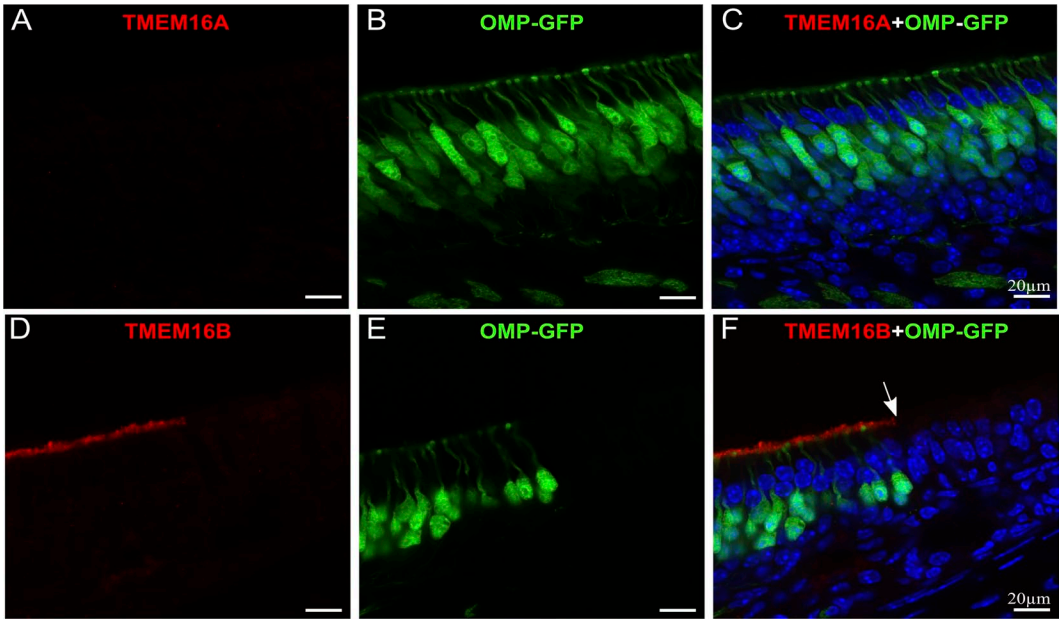

Figure 6. TMEM16A and TMEM16B immunoreactivity in the olfactory epithelium. (A–C) Confocal images of coronal sections of the olfactory epithelium from an OMP-GFP mouse showing the absence of TMEM16A immunoreactivity. (D–F) Confocal images of the transition region between the olfactory and the respiratory epithelium (absence of OMP-GFP–expressing neurons). The arrow indicates the transition between the two epithelia. TMEM16B is expressed at the apical surface of the olfactory but not of the respiratory epithelium. Cell nuclei were stained by DAPI (blue). Bars, 20 µm.

vomeronasal cells, we were not able to clearly identify supporting cells; therefore, we cannot exclude the possibility that TMEM16A and/or TMEM16B are also expressed in microvilli of these cells.

The rodent VNO has two major neuronal populations, apical and basal neurons, characterized by their location in the VNO and by the expression of specific proteins and receptors (Berghard and Buck, 1996; Jia and Halpern, 1996; Ryba and Tirindelli, 1997; Lau and Cherry, 2000; Leinders-Zufall et al., 2004; Liberles et al., 2009; Rivière et al., 2009). Apical neurons are located near the lumen of the VNO and express the G protein α subunit Gαi2, the PDE4A, and receptors of the V1R or formyl peptide receptor family. Basal neurons are close to the basal lamina and express the G protein α subunit Gαo and receptors of the V2R or formyl peptide receptor family. The finding that TMEM16A and TMEM16B are expressed in the microvilli of neurons raises the question of whether the expression of these proteins is restricted to any of these two neuronal subsets. We used specific markers to identify whether neurons expressing TMEM16A or TMEM16B are basal or apical. We performed immunocytochemistry on isolated vomeronasal sensory neurons using rabbit anti-PDE4A antibody, a marker for apical neurons, or rabbit anti-Gαo antibody, a marker for basal neurons (Lau and Cherry, 2000; Leinders-Zufall et al., 2004), together with the guinea pig anti-TMEM16A or anti-TMEM16B. Fig. 10 shows that TMEM16A and TMEM16B are localized in the microvilli of both apical (Fig. 10, A–C and G–I) and basal (Fig. 10, D–F and J–L) vomeronasal sensory neurons from wild-type mice. These results show that TMEM16A and TMEM16B are expressed in microvilli of both the apical and basal neuronal populations.

DISCUSSION

In this study, we have provided the first direct demonstration that a large Cl^- current can be directly activated by Ca^{2+} in the apical region of mouse vomeronasal sensory neurons. Indeed, photolysis of caged Ca^{2+} allowed us to obtain a precise temporal and spatial control of cytoplasmic Ca^{2+} elevation while recording the current in the whole cell voltage-clamp mode. Moreover, we have demonstrated that TMEM16A and TMEM16B largely colocalize with TRPC2 at the apical surface of the vomeronasal epithelium, and that TMEM16A and TMEM16B are coexpressed in microvilli of both apical and basal isolated vomeronasal sensory neurons, therefore suggesting that these two anion channels are likely to be involved in vomeronasal transduction.

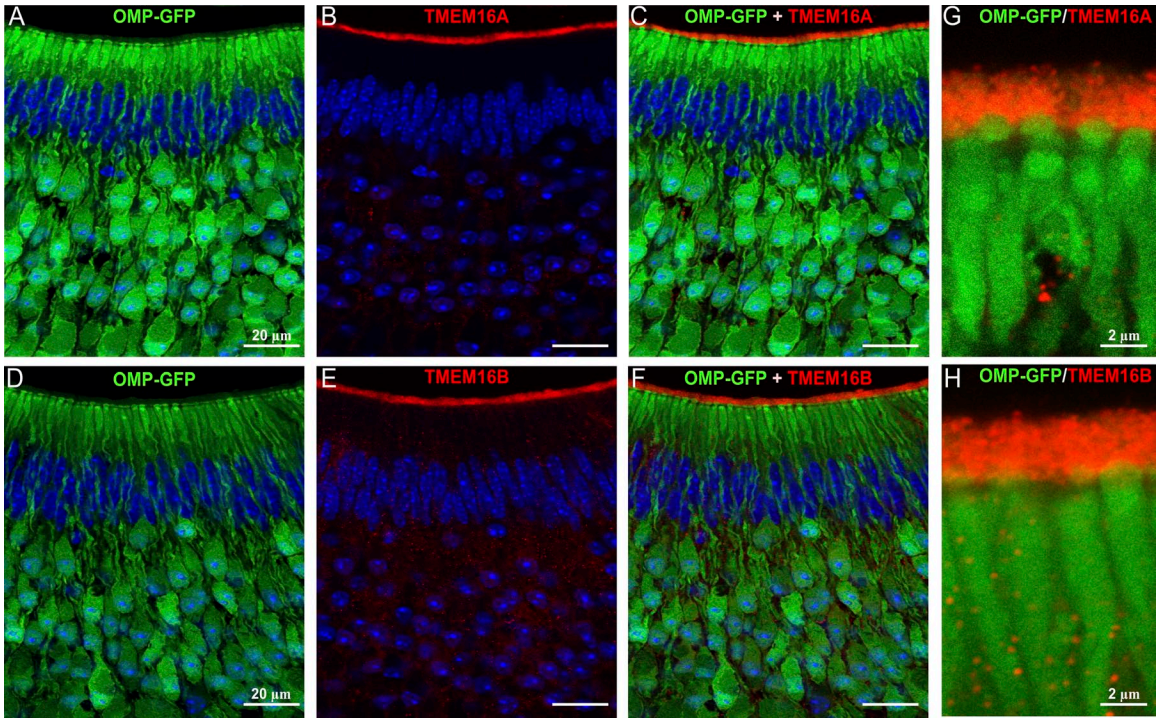

Figure 7. TMEM16A and TMEM16B are expressed at the apical surface of the vomeronasal epithelium. (A–H) Immunostaining of sections of VNO from an OMP-GFP mouse. (A and D) Endogenous GFP fluorescence of mature vomeronasal sensory neurons. TMEM16A (B) and TMEM16B (E) are expressed at the luminal surface of the vomeronasal sensory epithelium. (G and H) High magnification image of the apical portion of the VNO showing that TMEM16A and TMEM16B are expressed at the apical surface. Cell nuclei were stained by DAPI (blue). Bars: (A–F) 20 µm; (G and H) 2 µm.

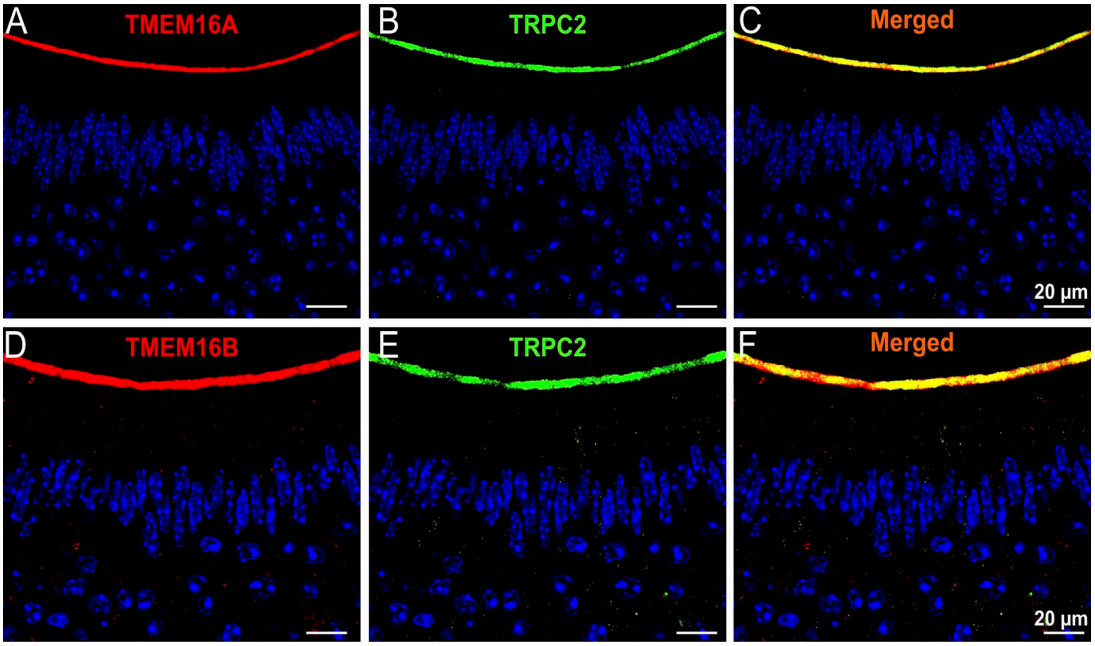

Figure 8. TMEM16A and TMEM16B are coexpressed with TRPC2. Double-label immunohistochemistry in tissue sections of VNO from a wild-type mouse showing the coexpression of TRPC2 with TMEM16A (A–C) and TMEM16B (D–F) at the luminal surface of the vomeronasal sensory epithelium. Cell nuclei were stained by DAPI (blue). Bars, 20 µm.

Expression of TMEM16A and TMEM16B in the vomeronasal epithelium

Two recent reports (Billig et al., 2011; Dauner et al., 2012) have shown that both TMEM16A and TMEM16B are expressed in the microvillar surface of the VNO. However, as pointed out by Dauner et al. (2012), the VNO apical surface layer contains the microvilli of both sensory neurons and supporting cells (Höfer et al., 2000). Thus, immunohistochemistry on coronal sections of the VNO does not allow for the distinction between these two microvillar subsets. By performing high resolution confocal imaging on isolated vomeronasal sensory neurons, we were able to detect both TMEM16A and TMEM16B in microvilli of the same neuron, thus providing the first unequivocal evidence of coexpression of these two anion channels in the same cell.

Ca^{2+}-activated currents in vomeronasal sensory neurons

Previous reports showed the presence of Ca^{2+}-activated nonselective cation currents in vomeronasal sensory

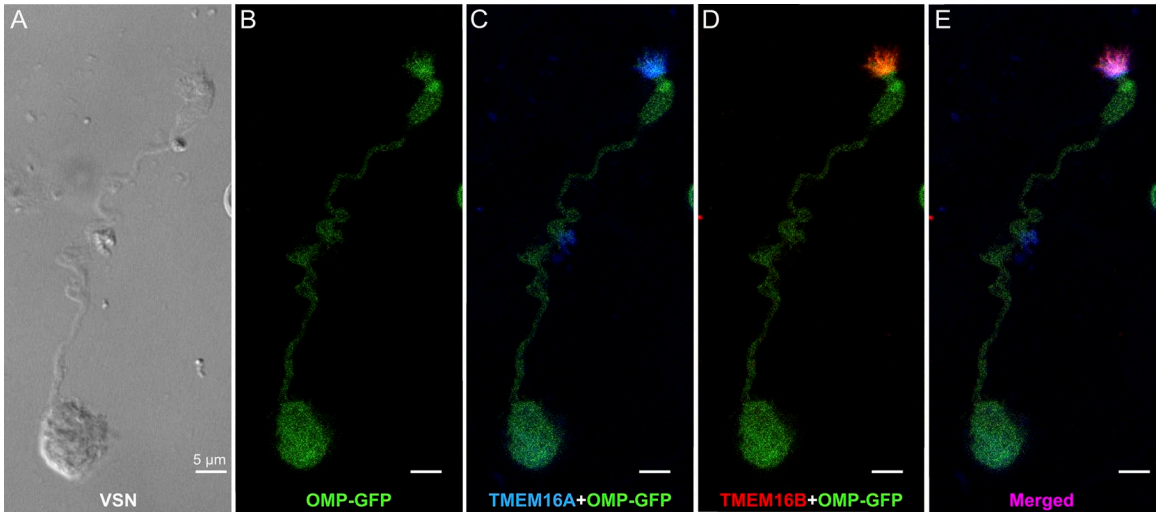

Figure 9. TMEM16A and TMEM16B are coexpressed in the microvilli of vomeronasal sensory neurons. (A) Bright field image of a vomeronasal sensory neuron isolated from an OMP-GFP mouse (B). The same neuron was stained with (C) rabbit anti-TMEM16A and (D) guinea pig anti-TMEM16B, showing the coexpression of the two anion channels in the microvilli (E). Cell nuclei were stained by DAPI (blue). Bars, 5 µm.

neurons (Liman, 2003; Spehr et al., 2009). In our experiments, with intracellular Cs^+ and extracellular Na^+ as the main monovalent cations, we did not detect any cation current. However, it must be pointed out that the anion and cation channels are likely to be activated in two very different ranges of Ca^{2+} concentration. Liman (2003) reported that half-activation of the nonselective cation channel occurred at a very high Ca^{2+} concentration: 0.5 mM at −80 mV. The Ca^{2+}-activated Cl^- channels TMEM16A and TMEM16B, located in the microvilli of vomeronasal sensory neurons, are half-activated at <5 µM (Pifferi et al., 2009a; Stephan et al., 2009; Xiao et al., 2011), a Ca^{2+} concentration that is 100-fold lower than that required to activate the nonselective cation currents. Moreover, although we did not directly measure the Ca^{2+} concentration photoreleased in the microvilli, estimates from our previous studies in olfactory sensory neurons obtained by comparing the normalized currents at various flash intensities (Boccaccio et al., 2006) with the dose–response relation for the native olfactory Ca^{2+}-activated Cl^- channels (Pifferi et al., 2009b) indicate that the maximal photoreleased concentration of Ca^{2+} is likely to be ∼10–20 µM. Thus, a Ca^{2+} concentration range lower than that necessary to activate the nonselective cation channels may explain the lack of detectable cation currents in our experiments.

Liman (2003) also stimulated inside-out patches from dendritic knobs of hamster vomeronasal sensory neurons with 2 mM Ca^{2+} and showed that the activated current was almost entirely cationic. Similar results were obtained by Spehr et al. (2009) by activating patches from mouse VNO neurons with 50 µM Ca^{2+}. It is likely that the explanation of the absence of the chloride component in these inside-out experiments is related to a rapid decrease of the current. Indeed, it has been shown that Ca^{2+}-activated Cl^- channels have a fast run-down in activity after patch excision from the dendritic knob of rat olfactory sensory neurons (Reisert et al., 2003) and that a detectable chloride current is present only in 75% of the patches from mouse olfactory sensory neurons (Fig. 6 C of Pifferi et al., 2009b).

A few recent studies have also provided some evidence for the presence of Ca^{2+}-activated Cl^- channels in vomeronasal sensory neurons. Yang and Delay (2010) used the perforated patch-clamp recordings with gramicidin, a technique that does not modify the intracellular Cl^- concentration, and demonstrated that 80% of the urine-induced current was carried by Ca^{2+}-activated Cl^- channels. These authors also showed that Ca^{2+} influx is

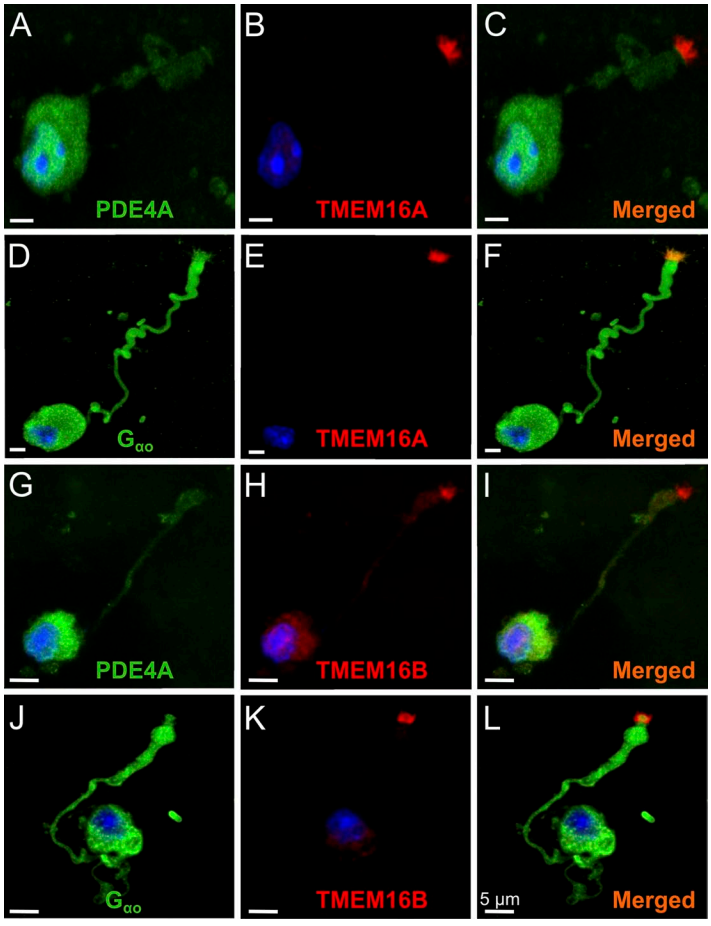

Figure 10. TMEM16A and TMEM16B are expressed in the microvilli of both apical and basal vomeronasal sensory neurons. TMEM16A (guinea pig antibody) is expressed in the microvilli of both apical neurons, as shown by PDE4A (A–C) immunoreactivity, and basal neurons, labeled with rabbit anti-Gαo antibody (D–F). TMEM16B (guinea pig antibody) is also located in the microvilli of both apical (G–I) and basal (J–L) neurons. Cell nuclei were stained by DAPI (blue). Bars, 5 µm.

necessary to activate the Cl^- channels. In another study, Kim et al. (2011) confirmed the previous study of Yang and Delay (2010) showing that a Ca^{2+}-activated Cl^- current contributes to urine response, but they also suggested that this current can be activated both by Ca^{2+} influx through the TRPC2 channel and by Ca^{2+} release from intracellular stores. Indeed, they also showed that knockout mice for TRPC2 still have a Ca^{2+}-activated Cl^- component in the response to urine that is blocked by compounds that inhibit intracellular Ca^{2+} release, thus suggesting that a TRPC2-independent signaling pathway may be operating in the VNO and that the Ca^{2+}-activated Cl^- current may play a relevant role in transduction.

Billig et al. (2011) compared whole cell recordings in vomeronasal sensory neurons from wild-type ($n = 7$) or knockout mice for TMEM16B ($Ano2^{-/-}$; $n = 6$) obtained with 1.5 µM Ca^{2+} or 0 Ca^{2+} in the pipette and reported that "currents of most $Ano2^{-/-}$ VSNs were indistinguishable from those we observed without Ca^{2+} (Fig. 5n), but a few cells showed currents up to twofold larger. Averaged current/voltage curves revealed that Ca^{2+}-activated Cl^- currents of VSNs depend predominantly on Ano2 (Fig. 5l). Although Ano1 is expressed in the VNO (Fig. 3a), its contribution to VSN currents seems minor." Thus, although most of the Ca^{2+}-activated current was abolished in knockout mice for TMEM16B, a residual current was still present in some neurons. It is likely that the residual current is carried by TMEM16A channels. Indeed, both TMEM16A and TMEM16B are known to independently function as Ca^{2+}-activated Cl^- channels (Scudieri et al., 2012), and we have demonstrated that TMEM16A and TMEM16B coexpress in microvilli of vomeronasal sensory neurons. Further experiments are necessary to unequivocally establish the origin of the residual current and to determine whether TMEM16A and TMEM16B form heteromeric channels and, if so, what the functional properties of the heteromeric channels are.

Physiological role of Ca^{2+}-activated Cl^- channels in vomeronasal and olfactory transduction

What is, then, the physiological role of Ca^{2+}-activated Cl^- channels in vomeronasal sensory neurons? Depending on the Cl^- equilibrium potential, these channels may contribute to the neuron depolarization or hyperpolarization. In vomeronasal sensory neurons, estimates of the Cl^- concentration inside the neurons and in the fluid filling its lumen are not available yet. However, experiments with the perforated patch-clamp recordings with gramicidin showed that the Ca^{2+}-activated Cl^- current acts to further amplify a primary inward depolarizing current (Yang and Delay, 2010), indicating that the intracellular Cl^- concentration was relatively high. In addition, the same authors showed that bumetanide, a specific blocker for the sodium potassium–chloride cotransporter NKCC1, significantly decreased the urine-induced inward current, indicating that NKCC1 is involved in chloride accumulation.

In olfactory sensory neurons, direct measurements of Cl^- concentrations showed that these neurons maintain an unusually high internal concentration of Cl^- of ~50 mM, which is similar to the Cl^- concentration present in the mucus at the external side of the ciliary membrane (Reuter et al., 1998; Kaneko et al., 2001, 2004). Therefore, in physiological conditions, the opening of Ca^{2+}-activated Cl^- channels causes an efflux of Cl^- ions from the cilia, which contributes to neuron depolarization. Up to 80% of the transduction current can be carried by Cl^-. Furthermore, studies from several laboratories indicated that TMEM16B is the main constituent of the Ca^{2+}-activated Cl^- channels involved in olfactory transduction. Indeed, it has been shown that TMEM16B is expressed in the ciliary layer of the olfactory epithelium, that currents in olfactory sensory neurons and in HEK 293T cells transfected with TMEM16B have very similar characteristics, and that knockout mice for TMEM16B did not show any detectable Ca^{2+}-activated Cl^- current (Pifferi et al., 2012). However, Billig et al. (2011) found that disruption of TMEM16B did not reduce mouse performance in some classical olfactory behavioral tasks, suggesting that Ca^{2+}-activated Cl^- channels may be dispensable for near-normal olfaction. Future experiments will have to establish whether Ca^{2+}-activated Cl^- channels are involved in more subtle aspects of olfactory sensing not detected in previous experiments.

It is of interest to note that, despite their differences in the molecular mechanisms of transduction, both olfactory and vomeronasal neurons express members of the TMEM16 family at the site of transduction, indicating that these channels are likely to play a physiological role in sensory transduction.

Conclusions

Our data contribute to the present understanding of the molecular mechanisms of vomeronasal transduction by providing the first direct evidence of the presence of a large Ca^{2+}-activated Cl^- current in the apical region of mouse vomeronasal sensory neurons and of the coexpression of the two Ca^{2+}-activated Cl^- channels TMEM16A and TMEM16B in the microvilli of the same sensory neurons. These observations suggest that TMEM16A and TMEM16B are likely to be responsible for the Cl^- current reported in this work.

In conclusion, collectively with previous studies indicating the presence of a Ca^{2+}-activated Cl^- component in urine response (Yang and Delay, 2010; Kim et al., 2011), our results contribute to the indication that Ca^{2+}-activated Cl^- channels could play a role in vomeronasal transduction. Future studies in mice in which the TMEM16A and/or TMEM16B gene are deleted will increase our understanding of the role of intracellular Ca^{2+} elevation in vomeronasal transduction.

We thank Stephan Frings (Heidelberg University, Heidelberg, Germany) for providing guinea pig antibodies against TMEM16A and TMEM16B, Peter Mombaerts (Max Planck Institute of Biophysics, Frankfurt, Germany) for providing OMP-GFP mice, Johannes Reisert for helpful discussions, Simone Pifferi and Anna Boccaccio for comments on the manuscript, and all members of the laboratories for discussions.

This study was supported by grants from the Italian Ministry of Education, University and Research, and from the Italian Institute of Technology.

Edward N. Pugh Jr. served as editor.

Submitted: 2 February 2012
Accepted: 6 June 2012

REFERENCES

Arnson, H.A., X. Fu, and T.E. Holy. 2010. Multielectrode array recordings of the vomeronasal epithelium. *J. Vis. Exp.* 1845.

Barry, P.H. 1994. JPCalc, a software package for calculating liquid junction potential corrections in patch-clamp, intracellular, epithelial and bilayer measurements and for correcting junction potential measurements. *J. Neurosci. Methods.* 51:107–116. http://dx.doi.org/10.1016/0165-0270(94)90031-0

Berghard, A., and L.B. Buck. 1996. Sensory transduction in vomeronasal neurons: evidence for G alpha o, G alpha i2, and adenylyl cyclase II as major components of a pheromone signaling cascade. *J. Neurosci.* 16:909–918.

Billig, G.M., B. Pál, P. Fidzinski, and T.J. Jentsch. 2011. Ca^{2+}-activated Cl^- currents are dispensable for olfaction. *Nat. Neurosci.* 14:763–769. http://dx.doi.org/10.1038/nn.2821

Boccaccio, A., and A. Menini. 2007. Temporal development of cyclic nucleotide-gated and Ca^{2+} -activated Cl^- currents in isolated mouse olfactory sensory neurons. *J. Neurophysiol.* 98:153–160. http://dx.doi.org/10.1152/jn.00270.2007

Boccaccio, A., L. Lagostena, V. Hagen, and A. Menini. 2006. Fast adaptation in mouse olfactory sensory neurons does not require the activity of phosphodiesterase. *J. Gen. Physiol.* 128:171–184. http://dx.doi.org/10.1085/jgp.200609555

Boccaccio, A., C. Sagheddu, and A. Menini. 2011. Flash photolysis of caged compounds in the cilia of olfactory sensory neurons. *J. Vis. Exp.* e3195.

Brennan, P.A. 2009. Pheromones and mammalian behavior. *In* The Neurobiology of Olfaction. A. Menini, editor. CRC Press, Boca Raton, FL. 157–179.

Brennan, P.A., and F. Zufall. 2006. Pheromonal communication in vertebrates. *Nature.* 444:308–315. http://dx.doi.org/10.1038/nature05404

Caputo, A., E. Caci, L. Ferrera, N. Pedemonte, C. Barsanti, E. Sondo, U. Pfeffer, R. Ravazzolo, O. Zegarra-Moran, and L.J.V. Galietta. 2008. TMEM16A, a membrane protein associated with calcium-dependent chloride channel activity. *Science.* 322:590–594. http://dx.doi.org/10.1126/science.1163518

Chamero, P., T.F. Marton, D.W. Logan, K. Flanagan, J.R. Cruz, A. Saghatelian, B.F. Cravatt, and L. Stowers. 2007. Identification of protein pheromones that promote aggressive behaviour. *Nature.* 450:899–902. http://dx.doi.org/10.1038/nature05997

Dauner, K., J. Lissmann, S. Jeridi, S. Frings, and F. Möhrlen. 2012. Expression patterns of anoctamin 1 and anoctamin 2 chloride channels in the mammalian nose. *Cell Tissue Res.* 347:327–341. http://dx.doi.org/10.1007/s00441-012-1324-9

Dean, D.M., A. Mazzatenta, and A. Menini. 2004. Voltage-activated current properties of male and female mouse vomeronasal sensory neurons: sexually dichotomous? *J. Comp. Physiol. A Neuroethol. Sens. Neural Behav. Physiol.* 190:491–499. http://dx.doi.org/10.1007/s00359-004-0513-8

Dibattista, M., A. Mazzatenta, F. Grassi, R. Tirindelli, and A. Menini. 2008. Hyperpolarization-activated cyclic nucleotide-gated channels in mouse vomeronasal sensory neurons. *J. Neurophysiol.* 100:576–586. http://dx.doi.org/10.1152/jn.90263.2008

Fieni, F., V. Ghiaroni, R. Tirindelli, P. Pietra, and A. Bigiani. 2003. Apical and basal neurones isolated from the mouse vomeronasal organ differ for voltage-dependent currents. *J. Physiol.* 552:425–436. http://dx.doi.org/10.1113/jphysiol.2003.052035

Frings, S. 2009a. Chloride-based signal amplification in olfactory sensory neurons. *In* Physiology and Pathology of Chloride Transporters and Channels in the Nervous System. From Molecules to Diseases. F. J. Alvarez-Leefmans and E. Delpire, editors. Elsevier-Academic Press, San Diego, CA. 413–424.

Frings, S. 2009b. Primary processes in sensory cells: current advances. *J. Comp. Physiol. A Neuroethol. Sens. Neural Behav. Physiol.* 195:1–19. http://dx.doi.org/10.1007/s00359-008-0389-0

Frings, S., D. Reuter, and S.J. Kleene. 2000. Neuronal Ca^{2+}-activated Cl^- channels—homing in on an elusive channel species. *Prog. Neurobiol.* 60:247–289. http://dx.doi.org/10.1016/S0301-0082(99)00027-1

Hartzell, C., I. Putzier, and J. Arreola. 2005. Calcium-activated chloride channels. *Annu. Rev. Physiol.* 67:719–758. http://dx.doi.org/10.1146/annurev.physiol.67.032003.154341

Hengl, T., H. Kaneko, K. Dauner, K. Vocke, S. Frings, and F. Möhrlen. 2010. Molecular components of signal amplification in olfactory sensory cilia. *Proc. Natl. Acad. Sci. USA.* 107:6052–6057. http://dx.doi.org/10.1073/pnas.0909032107

Höfer, D., D.W. Shin, and D. Drenckhahn. 2000. Identification of cytoskeletal markers for the different microvilli and cell types of the rat vomeronasal sensory epithelium. *J. Neurocytol.* 29:147–156. http://dx.doi.org/10.1023/A:1026548020851

Holy, T.E., C. Dulac, and M. Meister. 2000. Responses of vomeronasal neurons to natural stimuli. *Science.* 289:1569–1572. http://dx.doi.org/10.1126/science.289.5484.1569

Jia, C., and M. Halpern. 1996. Subclasses of vomeronasal receptor neurons: differential expression of G proteins (Gi alpha 2 and G(o alpha)) and segregated projections to the accessory olfactory bulb. *Brain Res.* 719:117–128. http://dx.doi.org/10.1016/0006-8993(96)00110-2

Kaneko, H., T. Nakamura, and B. Lindemann. 2001. Noninvasive measurement of chloride concentration in rat olfactory receptor cells with use of a fluorescent dye. *Am. J. Physiol. Cell Physiol.* 280:C1387–C1393.

Kaneko, H., I. Putzier, S. Frings, U.B. Kaupp, and T. Gensch. 2004. Chloride accumulation in mammalian olfactory sensory neurons. *J. Neurosci.* 24:7931–7938. http://dx.doi.org/10.1523/JNEUROSCI.2115-04.2004

Kim, S., L. Ma, and C.R. Yu. 2011. Requirement of calcium-activated chloride channels in the activation of mouse vomeronasal neurons. *Nat Commun.* 2:365. http://dx.doi.org/10.1038/ncomms1368

Kleene, S.J. 2008. The electrochemical basis of odor transduction in vertebrate olfactory cilia. *Chem. Senses.* 33:839–859. http://dx.doi.org/10.1093/chemse/bjn048

Lau, Y.E., and J.A. Cherry. 2000. Distribution of PDE4A and G(o) alpha immunoreactivity in the accessory olfactory system of the mouse. *Neuroreport.* 11:27–32. http://dx.doi.org/10.1097/00001756-200001170-00006

Leinders-Zufall, T., A.P. Lane, A.C. Puche, W. Ma, M.V. Novotny, M.T. Shipley, and F. Zufall. 2000. Ultrasensitive pheromone detection by mammalian vomeronasal neurons. *Nature.* 405:792–796. http://dx.doi.org/10.1038/35015572

Leinders-Zufall, T., P. Brennan, P. Widmayer, P.C. S, A. Maul-Pavicic, M. Jäger, X.H. Li, H. Breer, F. Zufall, and T. Boehm. 2004. MHC class I peptides as chemosensory signals in the vomeronasal organ. *Science.* 306:1033–1037. http://dx.doi.org/10.1126/science.1102818

Leinders-Zufall, T., T. Ishii, P. Mombaerts, F. Zufall, and T. Boehm. 2009. Structural requirements for the activation of vomeronasal sensory neurons by MHC peptides. *Nat. Neurosci.* 12:1551–1558. http://dx.doi.org/10.1038/nn.2452

Liberles, S.D., L.F. Horowitz, D. Kuang, J.J. Contos, K.L. Wilson, J. Siltberg-Liberles, D.A. Liberles, and L.B. Buck. 2009. Formyl peptide receptors are candidate chemosensory receptors in the vomeronasal organ. *Proc. Natl. Acad. Sci. USA.* 106:9842–9847. http://dx.doi.org/10.1073/pnas.0904464106

Liman, E.R. 2003. Regulation by voltage and adenine nucleotides of a Ca^{2+}-activated cation channel from hamster vomeronasal sensory neurons. *J. Physiol.* 548:777–787. http://dx.doi.org/10.1113/jphysiol.2002.037119

Liman, E.R., and D.P. Corey. 1996. Electrophysiological characterization of chemosensory neurons from the mouse vomeronasal organ. *J. Neurosci.* 16:4625–4637.

Liman, E.R., D.P. Corey, and C. Dulac. 1999. TRP2: a candidate transduction channel for mammalian pheromone sensory signaling. *Proc. Natl. Acad. Sci. USA.* 96:5791–5796. http://dx.doi.org/10.1073/pnas.96.10.5791

Ma, M. 2009. Multiple olfactory subsystems convey various sensory signals. *In* The Neurobiology of Olfaction. A. Menini, editor. CRC Press, Boca Raton, FL. 225–240.

Munger, S.D., T. Leinders-Zufall, and F. Zufall. 2009. Subsystem organization of the mammalian sense of smell. *Annu. Rev. Physiol.* 71:115–140. http://dx.doi.org/10.1146/annurev.physiol.70.113006.100608

Pifferi, S., A. Boccaccio, and A. Menini. 2006. Cyclic nucleotide-gated ion channels in sensory transduction. *FEBS Lett.* 580:2853–2859. http://dx.doi.org/10.1016/j.febslet.2006.03.086

Pifferi, S., M. Dibattista, and A. Menini. 2009a. TMEM16B induces chloride currents activated by calcium in mammalian cells. *Pflugers Arch.* 458:1023–1038. http://dx.doi.org/10.1007/s00424-009-0684-9

Pifferi, S., M. Dibattista, C. Sagheddu, A. Boccaccio, A. Al Qteishat, F. Ghirardi, R. Tirindelli, and A. Menini. 2009b. Calcium-activated chloride currents in olfactory sensory neurons from mice lacking bestrophin-2. *J. Physiol.* 587:4265–4279. http://dx.doi.org/10.1113/jphysiol.2009.176131

Pifferi, S., V. Cenedese, and A. Menini. 2012. Anoctamin 2/TMEM16B: a calcium-activated chloride channel in olfactory transduction. *Exp. Physiol.* 97:193–199.

Potter, S.M., C. Zheng, D.S. Koos, P. Feinstein, S.E. Fraser, and P. Mombaerts. 2001. Structure and emergence of specific olfactory glomeruli in the mouse. *J. Neurosci.* 21:9713–9723.

Rasche, S., B. Toetter, J. Adler, A. Tschapek, J.F. Doerner, S. Kurtenbach, H. Hatt, H. Meyer, B. Warscheid, and E.M. Neuhaus. 2010. Tmem16b is specifically expressed in the cilia of olfactory sensory neurons. *Chem. Senses.* 35:239–245. http://dx.doi.org/10.1093/chemse/bjq007

Reisert, J., and H. Zhao. 2011. Perspectives on: Information and coding in mammalian sensory physiology: Response kinetics of olfactory receptor neurons and the implications in olfactory coding. *J. Gen. Physiol.* 138:303–310. http://dx.doi.org/10.1085/jgp.201110645

Reisert, J., P.J. Bauer, K.W. Yau, and S. Frings. 2003. The Ca-activated Cl channel and its control in rat olfactory receptor neurons. *J. Gen. Physiol.* 122:349–363. http://dx.doi.org/10.1085/jgp.200308888

Reuter, D., K. Zierold, W.H. Schröder, and S. Frings. 1998. A depolarizing chloride current contributes to chemoelectrical transduction in olfactory sensory neurons in situ. *J. Neurosci.* 18:6623–6630.

Rivière, S., L. Challet, D. Fluegge, M. Spehr, and I. Rodriguez. 2009. Formyl peptide receptor-like proteins are a novel family of vomeronasal chemosensors. *Nature.* 459:574–577. http://dx.doi.org/10.1038/nature08029

Ryba, N.J., and R. Tirindelli. 1997. A new multigene family of putative pheromone receptors. *Neuron.* 19:371–379. http://dx.doi.org/10.1016/S0896-6273(00)80946-0

Sagheddu, C., A. Boccaccio, M. Dibattista, G. Montani, R. Tirindelli, and A. Menini. 2010. Calcium concentration jumps reveal dynamic ion selectivity of calcium-activated chloride currents in mouse olfactory sensory neurons and TMEM16b-transfected HEK 293T cells. *J. Physiol.* 588:4189–4204. http://dx.doi.org/10.1113/jphysiol.2010.194407

Schild, D., and D. Restrepo. 1998. Transduction mechanisms in vertebrate olfactory receptor cells. *Physiol. Rev.* 78:429–466.

Schroeder, B.C., T. Cheng, Y.N. Jan, and L.Y. Jan. 2008. Expression cloning of TMEM16A as a calcium-activated chloride channel subunit. *Cell.* 134:1019–1029. http://dx.doi.org/10.1016/j.cell.2008.09.003

Scudieri, P., E. Sondo, L. Ferrera, and L.J. Galietta. 2012. The anoctamin family: TMEM16A and TMEM16B as calcium-activated chloride channels. *Exp. Physiol.* 97:177–183. http://dx.doi.org/10.1113/expphysiol.2011.058198

Shimazaki, R., A. Boccaccio, A. Mazzatenta, G. Pinato, M. Migliore, and A. Menini. 2006. Electrophysiological properties and modeling of murine vomeronasal sensory neurons in acute slice preparations. *Chem. Senses.* 31:425–435. http://dx.doi.org/10.1093/chemse/bjj047

Spehr, M., H. Hatt, and C.H. Wetzel. 2002. Arachidonic acid plays a role in rat vomeronasal signal transduction. *J. Neurosci.* 22:8429–8437.

Spehr, J., S. Hagendorf, J. Weiss, M. Spehr, T. Leinders-Zufall, and F. Zufall. 2009. Ca^{2+}-calmodulin feedback mediates sensory adaptation and inhibits pheromone-sensitive ion channels in the vomeronasal organ. *J. Neurosci.* 29:2125–2135. http://dx.doi.org/10.1523/JNEUROSCI.5416-08.2009

Stephan, A.B., E.Y. Shum, S. Hirsh, K.D. Cygnar, J. Reisert, and H. Zhao. 2009. ANO2 is the cilial calcium-activated chloride channel that may mediate olfactory amplification. *Proc. Natl. Acad. Sci. USA.* 106:11776–11781. http://dx.doi.org/10.1073/pnas.0903304106

Stöhr, H., J.B. Heisig, P.M. Benz, S. Schöberl, V.M. Milenkovic, O. Strauss, W.M. Aartsen, J. Wijnholds, B.H.F. Weber, and H.L. Schulz. 2009. TMEM16B, a novel protein with calcium-dependent chloride channel activity, associates with a presynaptic protein complex in photoreceptor terminals. *J. Neurosci.* 29:6809–6818. http://dx.doi.org/10.1523/JNEUROSCI.5546-08.2009

Tirindelli, R., M. Dibattista, S. Pifferi, and A. Menini. 2009. From pheromones to behavior. *Physiol. Rev.* 89:921–956. http://dx.doi.org/10.1152/physrev.00037.2008

Touhara, K., and L.B. Vosshall. 2009. Sensing odorants and pheromones with chemosensory receptors. *Annu. Rev. Physiol.* 71:307–332. http://dx.doi.org/10.1146/annurev.physiol.010908.163209

Xiao, Q., K. Yu, P. Perez-Cornejo, Y. Cui, J. Arreola, and H.C. Hartzell. 2011. Voltage- and calcium-dependent gating of TMEM16A/Ano1 chloride channels are physically coupled by the first intracellular loop. *Proc. Natl. Acad. Sci. USA.* 108:8891–8896. http://dx.doi.org/10.1073/pnas.1102147108

Yang, C., and R.J. Delay. 2010. Calcium-activated chloride current amplifies the response to urine in mouse vomeronasal sensory neurons. *J. Gen. Physiol.* 135:3–13. http://dx.doi.org/10.1085/jgp.200910265

Yang, Y.D., H. Cho, J.Y. Koo, M.H. Tak, Y. Cho, W.-S. Shim, S.P. Park, J. Lee, B. Lee, B.-M. Kim, et al. 2008. TMEM16A confers receptor-activated calcium-dependent chloride conductance. *Nature.* 455:1210–1215. http://dx.doi.org/10.1038/nature07313

Zufall, F., K. Ukhanov, P. Lucas, E.R. Liman, and T. Leinders-Zufall. 2005. Neurobiology of TRPC2: from gene to behavior. *Pflugers Arch.* 451:61–71.

Zufall, F., and T. Leinders-Zufall. 2007. Mammalian pheromone sensing. *Curr. Opin. Neurobiol.* 17:483–489. http://dx.doi.org/10.1016/j.conb.2007.07.012